Journal of Petroleum Science and Technology 13(4): 40, 2023, Pages 45-52
DOI:10.22078/jpst.2024.5144.1886

Journal of Petroleum Science and Technology
Research Paper
https://jpst.ripi.ir/

Modification of Sodium Montmorillonite: Dependence of Silylation on Premixing Process

Milad Fardi, Jamal Aalaie* and Sanam Sepehri
Chemical, Polymer and Petrochemical Technology Development Research Division, Research Institute of Petroleum Industry (RIPI), Tehran, Iran

Abstract

Organic modification of hydrophilic sodium montmorillonite (Na+-MMT) is important for improving its compatibility with organic polymers. In the present research, (3-aminopropyl)triethoxysilane (APTES) was used to modify Na$^+$-MMT. The effects on the basal spacing of Na$^+$-MMT upon the premixing process with different mixing techniques were examined in detail. The resultant products (S-Mts) were characterized by X-ray diffraction (XRD), thermogravimetric analysis (TGA), and Fourier transform infrared (FTIR) spectroscopy. For monitoring the grafting process, FTIR was used, while the percentage of the loaded silane was calculated using TGA. Furthermore, XRD measurements were carried out to evaluate the increase in the d-spacing. The amount of grafted silane increases when a suitable premixing process, such as the mechanical mixer and homogenizer, is chosen. The same beneficial effects were observed on d-spacing, as it increases when using the mechanical mixer and homogenizer. This study demonstrates that the degree of grafting and d-spacing of the grafted products strongly depends on the mixing process before the silylation reaction. This is very important for the synthesis and application of polymer nanocomposites containing silylated layered silicate minerals.

Keywords: Sodium montmorillonite, Silylation, Premixing process, Grafting reaction.

Introduction

Polymer/nanoclay nanocomposites have attracted much attention in the polymer industry due to their remarkable and improved properties. This area emerged with the recognition that exfoliated clays could show better thermal performance, higher strength, and barrier properties than virgin polymers or conventional micro/macro composites [1-4]. The more common clay used for preparing polymer/nanoclay nanocomposites belongs to the family of 2:1 layered or phyllosilicates and, more specifically, to the smectite group [5]. Among the smectite groups, sodium montmorillonite nanoclay (Na$^+$-MMT) is one of the most commonly used clays in polymer/nanoclay nanocomposites [6-8]. In Na$^+$-MMT structure, SiO_4^{4-} and $Al(OH)_6^{3-}$ are interconnected by the sharing of O^{2-} at polyhedral corners and edges in such a way that a sheet of tilted $Al(OH)_6^{3-}$ is sandwiched between two sheets of SiO_4^{4-} [9-10]. The thickness of the layer (interlayer spacing height) is 9.6 Å (without considering the height provided by the exchangeable cations, the thickness of the 2: 1 layer is approximately 7 Å), and stacking of these layers because of a regular Vander Waals gap between the layers make the gallery or interlayer [11]. The layers in the crystal plane are negatively charged. These negative charges are balanced by Na$^+$ cations within the interlayer space [12]. The interaction between Na$^+$-MMT particles and most organic polymers significantly depends on these net charges in the nanoclay particles [13]. Accordingly, because of the weak interfacial interactions between the hydrophobic polymeric chains and Na$^+$-MMT hydrophilic reaction sites, simply mixing Na$^+$-MMT in a polymer matrix would not make a composite with enhanced properties [13-14]. Therefore, less compatibility of clay with the organic polymers is one of the important problems in producing polymer/clay nanocomposite [5]. To render Na$^+$-MMT compatible with various polymer systems, the hydrophilic clay surface should be converted to an organophilic one [13,7,15]. On the other hand, some of the special functional groups (e.g., $-NH_2$ group) can react with the polymer matrix. It can considerably improve the mechanical properties of the resultant polymer/clay nanocomposite [15]. In this regard, various studies have been made to decrease the hydrophilicity of the Na$^+$-MMT internal platelets and modify the inorganic clay for better compatibility with polymers [6,16,13,11]. One of the most commonly used techniques to modify the clay surface is the cation exchange reaction with a quaternary

---

**Corresponding author:* Jamal Aalaie, Chemical, Polymer and Petrochemical Technology Development Research Division, Research Institute of Petroleum Industry (RIPI), Tehran, Iran
E-mail addresses: aalaiej@ripi.ir
Received 2023-08-06, Received in revised form 2024-01-27, Accepted 2024-02-12, Available online 2024-05-02

ammonium salt. This technique produces hydrophobic Na^+-MMT with a greater gallery space. Nevertheless, because of the quaternary ammonium salt degradation at high temperatures, the thermal instability of the organoclay becomes a strong limitation in the processing of polymer/clay nanocomposite [17]. Consequently, the silylation method (by using organosilanes) has attracted considerable interest from researchers. The grafting reaction is generally a modification of the material's surface by chemisorption, representing a usable procedure to produce a compatible organic matrix [15, 18-21]. Crystal defects (e.g., broken bonds) are usually present in layered silicates. It causes the formation of hydroxyl groups, which can be used for chemical grafting by a silylation reaction. Organic functional groups can covalently bond onto the layer surface by using an organosilane [22]. In particular, the molecular bond of the organosilane with the clay mineral can occur on three different sites: at the external surface (without altering the basal spacing), at the gallery space, and the edges (providing expansion of the basal spacing) [18,23]. The d-spacing of the modified products vigorously depended on three factors: 1- the interactions among organosilane molecules and between Na^+-MMT platelets and a particular group of organosilane (for example $-NH_2$ group), 2- the grafted amount of aminosilane of the interlayer spaces and 3- configuration of the organosilane used [18]. In some research, it is concluded that the silylation would enhance the interfacial interaction of polymer/nanoclay, and this interaction is more important than the clay morphology [24]. Most grafted products have been prepared by the reactions of reactive silane derivatives, which have also been applied to modify inorganic oxide nanoparticles and organic polymer chains [19]. So far, several research groups have focused on studying the effect of different factors such as aminosilane type [23-27], solvent nature [28], polar and non-polar solvents [29], temperature [30] and dispersing media [31] on the swelling of silylated clay minerals and the silylation mechanism. In these researches, the organic modification of nano clay is a very promising route since reactions can occur on the broken edges, the interlayer space, and the surface. The present work illustrates how the mixing process before the grafting reaction can be a key factor for forming the intercalated silane and good dispersion of the layers of silylated Na^+-MMT. In this study, the grafting of Na^+-MMT with (3-aminopropyl)triethoxysilane (APTES) and the characteristics of the resultant products using X-ray diffraction (XRD), thermogravimetric analysis (TGA) and Fourier transform infrared (FTIR) spectroscopy were reported. In the present study, the grafting reaction and premixing process were carried out in two separate steps, and the effect of the mixing process before the grafting of organosilane onto the Na^+-MMT surface was specifically considered. The d-spacing and the amount of the grafted silane were the two parameters studied thoroughly in this research. As far as we know, the effect of the premixing process on the silylation reaction and the Na^+-MMT final d-spacing has not been reported yet. For premixing, three different mixers were used: 1- A homogenizer that is a high shear mixer, 2- A sonicator in which sound waves are used to agitate particles in a solution, and 3- A mechanical mixer in which a blade stirrer was used for premixing. The results of this paper reveal that the premixing process can be an important factor in the increase of the swelling feature of the silylated Na^+-MMT and the improvement of the polymer/clay nanocomposite properties.

Materials and Methods

Commercial sodium montmorillonite (Cloisite Na^+) was provided by Southern Clay Products Inc. The cation exchange capacity (CEC) and specific gravity of clay were 92.6 meq/100 g and 2.86 g/cc, respectively. According to the manufacturer's information, the particle size of 90 vol% of dry clay is less than 13µ. Its general formula is $AlSi_2O_5(OH)\times H_2O$. Moreover, Na^+-MMT was dried overnight at 90°C in a vacuum oven before silylation. Furthermore, (3-Aminopropyl)triethoxysilane (APTES) was purchased from Merck Co. The trifunctional silylating agent with a purity of 98% was used as received. Throughout all the experiments, distilled water was used. Also, the Heidolph MR Hei-Tec magnetic stirrer, Heidolph Silent Crusher M homogenizer, Heidolph mechanical stirrer (RZR 2020), and ultrasonic (VGT-1990QTD) were used for premixing processes.

Silylation Reaction

Two different experimental steps were used to carry out the Na^+-MMT silylation reaction using 3-Aminopropyl) triethoxysilane. These two experimental steps, step 1 and step 2, are summarized in Table 1. At first, 1 g of the dried Na^+-MMT was dispersed in 100 mL of solvent (distilled water) at different mixing conditions for 15 min (the premixing process) at room temperature according to Table 1 (see step 1). Separately, APTES solution was prepared by dissolving 4 gr of APTES in 100 mL of distilled water at 1000 rpm for 15 min at 25°C. The prepared Na^+-MMT dispersion and APTES solution were then mixed, and the grafting reactions were performed according to Table 1 (see step 2). In this study water was selected as the solvent, since recent studies confirmed that using the solvents with high surface energy (like water) in the process of the clay mineral modifying makes the silane to diffuse easily into the mineral layers of clay and reacts more effectively in the galleries of the mineral [32].

Table 1 Premixing and reaction conditions adopted during the silylation process.

Sample	Step 1 (premixing)	Step 2 (reaction)
S-Mt0	--------	Magnetic mixer, 400 rpm, 4h, room temperature
S-MtU	Ultrasonic, 240W, 40 kHz	
S-MtHL	Homogenizer (7500 rpm)	
S-MtHH	Homogenizer (26000 rpm)	
S-MtME	Mechanical mixer (1000 rpm)	

Ahenach et al. also verified that when water is a solvent, it is possible that condensation and hydrolysis occur before intercalation [33]. It is worth noting that the reduced time and absence of heating during the functionalization in media containing only water are advantageous in economic terms [34]. In addition, Piscitelli et al. found that decreasing the Na^+-MMT interlayer distance is due to increasing the length of the organic chains of the silane modifiers. On the contrary, 3-aminotriethoxysilane molecules (compared to other aminosilanes) make a better screening between the charges of the Na^+-MMT layers and weaken the interlayer attraction forces; thereby, these silane molecules result in a larger basal spacing value [25]. For this reason, 3-aminotriethoxysilane was selected as a coupling agent. Furthermore, in this study, the high amount of aminosilane (4g) was used, because by increasing the concentration of aminosilane the quantity of aminosilanes able to penetrate into the Na^+-MMT gallery platelets increases, which would result in a higher enlargement of the basal spacing and a larger amount of intercalated grafted silane modifiers [25]. The reaction products were filtered and washed using distilled water and also in order to remove the excess silane centrifuged (at 15000 rpm) during 15 min. This washing procedure was repeated three times. Each resultant product was dried at 90°C for 24 hr under vacuum condition then ground to a powder. The modified clay mineral samples (S-Mts) in various premixing processes - the silylation reaction without the premixing process, ultrasonic mixing, homogenizer at 7500 RPM, homogenizer at 26000 rpm, magnetic mixer and mechanical mixer - were called S-Mt_0, S-Mt_U, S-Mt_{HL}, S-MtHH, S-M_{tM} and S-Mt_{ME}, respectively. For the purpose of study the effect of premixing process on the final products, the amount of the loaded silane and the interlayer spacings of the S-Mts obtained from the two procedures, were compared. In order to ensure the results, some tests were performed twice.

Instrumental Analyses

Fourier Transform Infrared Analysis

FTIR spectra were recorded by using an ALPHA FTIR spectrometer on KBr pressed pellets (about 1 mg of sample and 1 g of dry potassium bromide were mixed and pelletized in a hydraulic press at 10 kPa). FTIR spectra were collected over a range of 400-4000 cm^{-1}.

Thermogravimetric Analysis

TGA was carried out on a Mettler Toledo TGA SDTA 851 thermogravimetric analyzer. About 5 mg of the sample was heated in a closed platinum pan from 25 to 800°C at a heating rate of 10°C/min under nitrogen flow. The mass loss and the percentage of the loaded silane, which corresponds to the percentage of organic aminosilane moieties concerning the total inorganic mass, were calculated using the following equations (Equations 1 to 3) [35,18]:

$$Silane\ loaded\ amount\ (\%) = \frac{100 \times W_{200-600}}{100 - W_{(200-600)}} \times 100\% \tag{1}$$

$$Mass\ loss\ \ (\%) = W_{200-600} \times 100\% \tag{2}$$

$$Silane\ loaded\ amount\ \left(\frac{mequiv}{g}\right) = \frac{10^3 W_{200-600}}{(100 - W_{(200-600)})M} \tag{3}$$

where W200–600 and M (g/mol) correspond to the corrected mass loss between 200°C and 600°C and the molecular mass of the silane molecules, respectively. Due to the evaporation of water, pure Na^+-MMT reveals a mass loss in this region. Therefore, W200− 600 of pure Na^+-MMT was subtracted from the mass loss of the samples to give a correct value of W200− 600.

Wide Angle X-ray Diffraction Analysis

The basal spacing is defined as the interlayer space between the clay platelets, usually denoted as d-spacing or d001 [25]. To evaluate the increase in the basal spacing, XRD measurements were performed. XRD patterns were recorded on a Philips XPert PW1840 using a cobalt tube anode (λ= 0.178896 nm) under a voltage of 40 kV and a current of 25 mA. The basal spacings were calculated from the 2θ values using Bragg's equation, λ=2dsinθ (where λ is the wavelength of the X-ray (0.178896nm); θ is the diffraction angle; and d is the basal space between clay layers) [36]. The XRD patterns were recorded with a step size of 0.04° from 2θ=1 to 15° in a transmission mode.

Results and Discussion

Previous reports have revealed that OH groups on the broken edges, montmorillonite surface, and structural defects in the Si–O tetrahedral sheets are active and can undergo grafting reactions with 3-aminotriethoxysilane molecules [23]. In an aqueous solution, silane is easy to hydrolyze and condense among silane molecules as following reactions (I) and (II) (the functionality of the silane was not considered because of the simplification of the reactions) [27].

≡Si–OEt+H_2O→≡Si–OH+EtOH, (Hydrolysis. I)
≡Si–OH+OH–Si≡→≡Si–O–Si≡+H_2O. (Condensation.II)

The hydrolysis reaction involves replacing ethoxy groups (OEt) with hydroxyl groups (OH). Hydrolysis and condensation reactions occur before intercalation (Step 1), and after hydrolysis, the configuration of silane will be changed with polymerization [33]. In addition, when the single APTES molecules were intercalated into the Na^+-MMT interlayer space, the d-spacing will be a function of the amount of the intercalated organic molecules. In this case, silane hydrolysis and condensation occur after intercalation [27].

Fourier Transform Infrared Analysis

Fig. 1 exhibits an enlargement of the IR between 2600 and 4000 cm-1 for the Na^+-MMT, APTES, and S-Mts compounds. In FTIR analysis, we tried to use the same amounts of the functionalized Na^+-MMTs for all samples so that the intensity of the peaks could be compared accurately. All the spectra have been normalized to the peak height of the Na^+-MMT clay (Mt) at 1045 cm^{-1} to allow for the band intensity comparison. The peak at 3630 cm^{-1} corresponds to the stretching vibrations of the OH bound of magnesium (Al(Mg)OH) or aluminum (Al(Al)OH) of the Na^+-MMT. The possible presence of adsorbed water cannot be ruled out because the band due to the presence of water occurs at approximately 3420 cm^{-1}, and it is because of the stretching of the OH groups of the adsorbed water molecules intercalated in the clay mineral [18]. A shoulder at 3290 cm^{-1} in Fig. 1 may be assigned to the stretching of the NH_2 group [25].

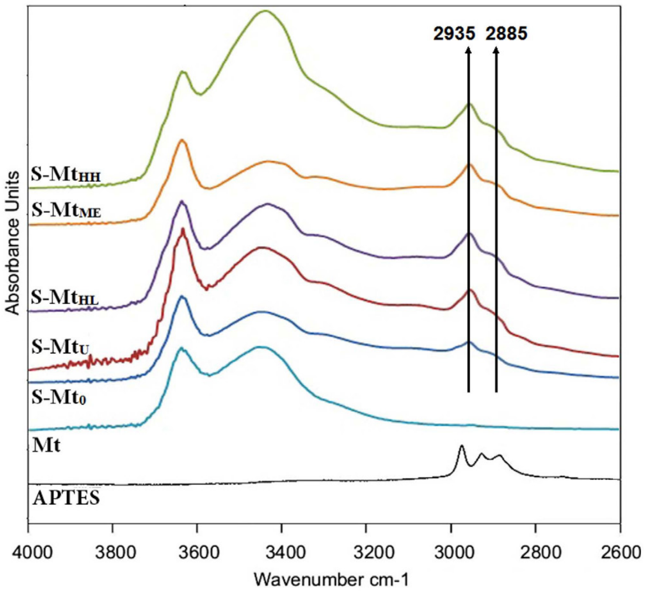

Fig. 1 FTIR spectra of APTES, pristine Na$^+$-MMT (Mt), S-Mt$_0$; S-Mt$_U$, S-Mt$_{HL}$; S-Mt$_{ME}$ and S-Mt$_{HH}$.

The presence of C–H and N–H absorbance peaks in the corresponding IR spectra is the main evidence for the successful intercalation silylation of the aminoalkyl silanes in the Na$^+$-MMT galleries, as pointed out by Zhao et al. [37]. In the same figure, the APTES and the fresh Na$^+$-MMT are also shown for comparison.In comparison with the neat Na$^+$-MMT spectrum, the five modified clay mineral samples show additional peaks which can be attributed to the antisymmetric and symmetric stretching vibrations of the methylene groups at 2935 and 2885 cm^{-1}, respectively, therefore confirming the presence of the organic moieties on the Na$^+$-MMT surface [25]. The intensities of the bands at 2885 and 2935 cm^{-1}, corresponding to the symmetric and antisymmetric stretching vibrations of –CH$_2$, increase for S-Mts compounds (Fig. 1). It is worth noting that, by using a suitable mixer, both NH$_2$ and CH$_2$ adsorption peaks in Fig. 1 become progressively more pronounced (for samples prepared by homogenizer and mechanical mixer, i.e., S-Mt$_{ME}$, S- Mt$_{HH}$ and S-Mt$_{HL}$, respectively), suggesting the presence of a larger amount of grafted silane modifiers. Here, it can be seen that the premixing process significantly influences the amount of grafted silanes.

Thermogravimetric Analysis

The S-Mts showed a weight loss greater than the Na$^+$-MMT, possibly due to organic compounds in the structure. In the case of S-Mts (Fig. 2), the weight loss below 100°C (the peak around 63°C) can be attributed to the vaporization of free water (between pores and aggregates) and water bonded to the cations by hydrogen bonding or free solvents present between the pores. The degradation in the temperature range from 200°C to 600°C is assigned to the thermal decomposition of silane molecules [18,32].

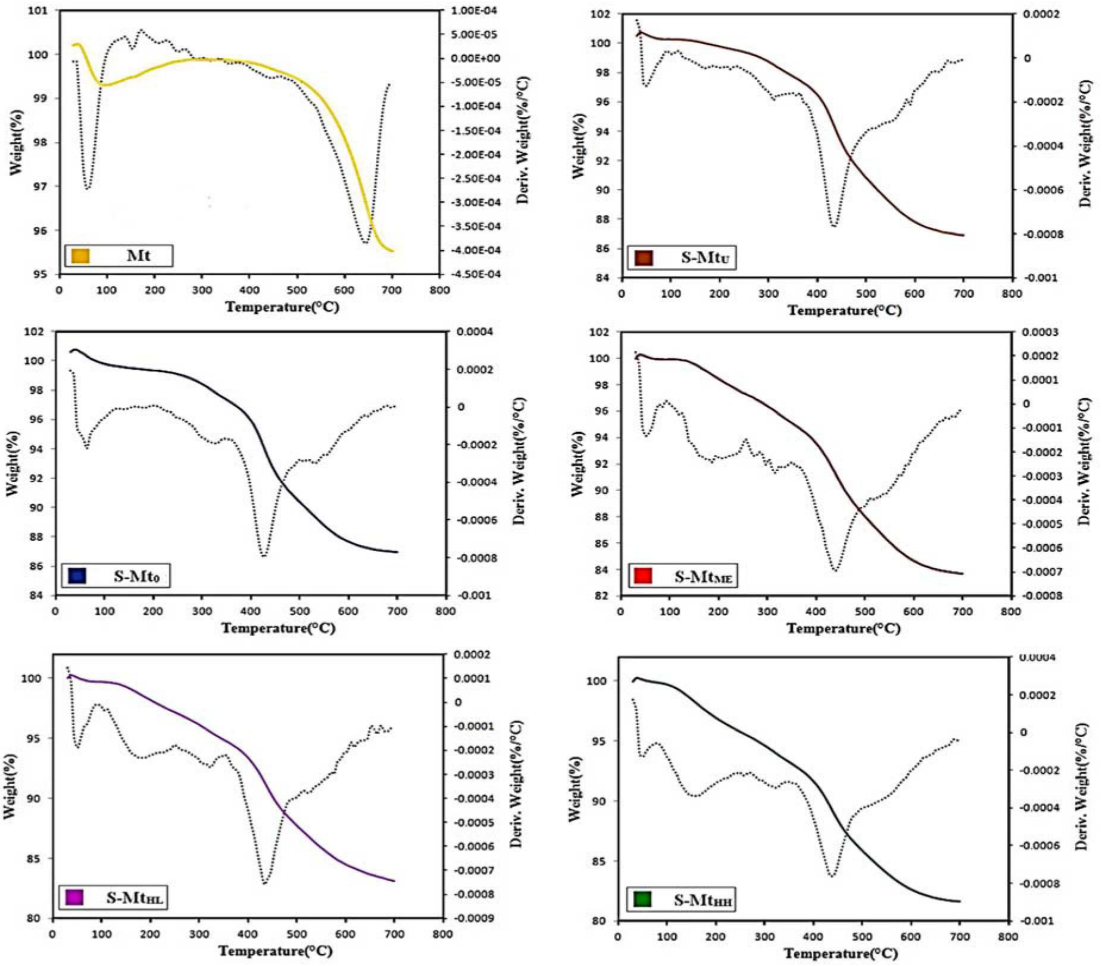

Fig. 2 TGA and DTGA curves (25-80°C) of pristine(Mt) and Modified Na$^+$-MMT(SMts).

However, for pristine Na^+-MMT, there is a small mass loss (ca. 4 wt %) in the range of 200–600 °C, possibly corresponding to the loss of the bonded water within the gallery. Consequently, a greater mass loss than expected is attributed to the grafted silane's decomposition and evaporation [23]. It provides another evidence for the chemical bonding between the siloxane surfaces of Na^+-MMT and silane. As reported in the literature, DTG curves of the S-Mts display four peaks in the 200–600 °C range, interpreted as the degradation of intercalated, physically adsorbed, and grafted silane molecules [18,37-38]. In Figure 2, three broad peaks were observed at ca. 180 °C, 310 °C and 430 °C, which were attributed to the silanes physisorbed on surfaces of Na^+-MMT, covalently bonded at the adsorbed or broken edges on the outer Na^+-MMT surfaces, and intercalated in the interlayer spaces, respectively. The mass loss at ca. 550 °C is assigned to the silane chemically bonded with the decomposition of the grafted aminosilanes or the layers of the Na^+-MMT [23,38-39]. The weight loss between 250 °C and 340 °C can be attributed to the covalently bonded at the broken edges of Na^+-MMT. In this case, the mass loss at around 420 °C shows the high amount of intercalated aminosilanes, and the broad peaks at 557 °C and 671 °C could be assigned to the chemically grafted silane with the clay platelets and the degradation of aluminum silicate layers, respectively [32]. The mass losses in the range of 200 °C and 600 °C were used as the entry parameters in Eq. 1 to Eq. 3 to evaluate the amounts of grafted aminosilane, and the corresponding results are shown in Table 2. As indicated by TGA measurements, the S-Mt_{HL}, S-Mt_{ME}, and S-Mt_{HH} revealed more silane in their structures, 13.62%, 13.85% and 14.56%, respectively. The lowest silane loaded, around 10.97%, was observed in S-Mt_0. It is worth noting that the main difference between the obtained products seems to be due to the amount of silane adsorbed and intercalated rather than the amount of grafted silane. However, from the DTG and TGA curves, it is clear that the premixing process influences the degree of surface adsorption, the amount of grafted silane molecules, and the intercalation of silane between the clay platelets.

Wide Angle X-ray Diffraction Results

To quantify the effect of the premixing process on the basal spacing of Na^+-MMT, silylation reactions were carried out using the three different premixing processes: ultrasonication, mechanical mixer and homogenizer. In XRD, the same amounts of the functionalized Na^+-MMTs for all samples were tested to compare the samples accurately. The patterns of X-ray diffraction related to the d-spacing (001), displayed in Fig. 3, demonstrate that compared to the pristine Na^+-MMT, the introduction of aminosilane into the Na^+-MMT gallery shifts the peak at lower 2θ values. In detail, an obvious increase of the d-spacing in the S-Mts was observed, from 15.22 Å (pristine Na^+-MMT) [6] to ca. 20.69 Å (S-Mt_{ME}) (Table 3).

Table 2 Percentage of silane loaded in the S-Mts as determined by the TGA.

Sample	mass lossa(%)	Grafting amount	
		(%)^b	(meq/g)^c
S-Mt0	9.88	10.97	0.495
S-MtU	10.22	11.38	0.514
S-MtHL	11.99	13.62	0.615
S-MtME	12.16	13.85	0.626
S-MtHH	12.71	14.56	0.658

a Determined by using Eq.(2).
b Determined by using Eq.(1).
c Determined by using Eq.(3).

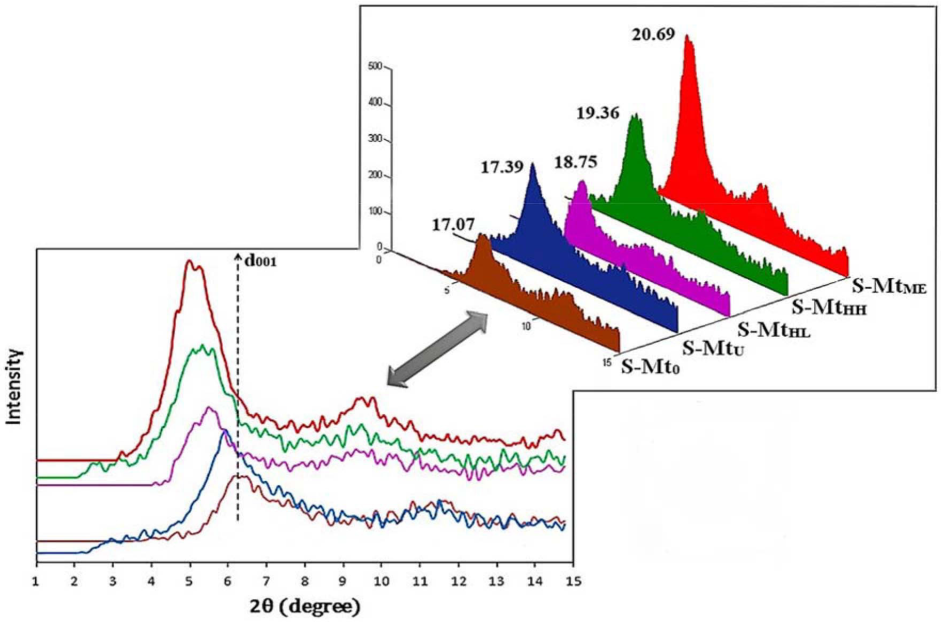

Fig. 3 X-ray diffraction patterns of the functionalized Na+-MMTs.

Table 3 d-Spacing values and the interlayer space height for Na$^+$-MMT and S-Mts.

Sample	2θ (degree)	Distance d001(Å) (Basal spacing)	Interlayer space height (Å)[a]
Na+-MMT	6.75	15.22	5.62
S-Mt0	6.16	16.67	7.07
S-MtU	5.92	17.35	7.75
S-MtHL	5.48	18.73	9.13
S-MtHH	5.32	19.30	9.70
S-MtME	4.96	20.69	11.09

a Determined by using Eq.(4).

This significant increase in basal spacing of 15.22 Å for values of up to 20.69 Å is a clear signal that the silane molecules have been grafted or intercalated at the edges of the Na$^+$-MMT or in the interlayer region [23,32,27]. Remarkably, the appearance of a second peak in some of the S-Mts reflects (002) [28]. Concerning the effect of the premixing process, S-Mt0 shows a lower basal spacing value (d001=16.67 Å) compared to the S-MtU (d001=17.35 Å), S-Mt$_{HL}$(d001=18.73 Å), S-Mt$_{HH}$ (d001=19.30 Å), and S-Mt$_{ME}$(d001=20.69). It could be concluded that the silylation reaction without the premixing process (S-Mt$_0$) has the smallest d-spacing compared with the other modified clay mineral samples (S-Mts). According to this observation, it is clear that to perform a good intercalation and grafting of silane molecules between clay layers, a premixing process is necessary.

Using Eq. 4, the interlayer spacing height (Å) can be estimated [18, 23, 27].

$$\text{Interlayer space height (Å)} = \text{Distance d001} - 9.6\ \text{Å} \qquad (4)$$

In this equation, 9.6 Å is the basal spacing of the sheet of phyllosilicate.

Table 3 shows the d-spacing values and the heights of the interlayer space for the S-Mts prepared using different premixing methods. The Na$^+$-MMT interlayer space has a height of approximately 5.62 Å and reached a maximum value of 11.09 Å after modification. According to the literature, after hydrolysis, the APTES configuration is different from the original one, and the aminopropyl group height is about 0.4 nm (~ 4 Å), similar to that of the alkyl chain [23]. Accordingly, the gallery heights of 7.47 Å and 7.79 Å indicate the monolayer arrangement of APTES within the galleries of S-Mt0 and S-MtU, respectively. The modified Na$^+$-MMTs that probably show a double layer of aminopropyl are S-Mt$_{HL}$, S-Mt$_{HH}$, and S-Mt$_{ME}$. Notably, when the clay mineral and water are mixed in the experiments, water first diffuses into the Na$^+$-MMT gallery and expands the clay layers [28].

The aminosilane is also mixed in water separately (step 1), and the hydrolysis and condensation reactions between some silane molecules take place [27]. Ultimately, the resulting Na$^+$-MMT dispersion and aminosilane solution are mixed, and the grafting reactions are performed (step 2). Recently, researchers found out that water facilitates the penetration of the siloxane oligomers or silane in the space between parallel platelet layers of the clay mineral [32,39]. Furthermore, using the higher quantity of aminosilanes (4g in this study), the amount of aminosilanes able to penetrate the platelets of the Na$^+$-MMT gallery increases, and a higher enlargement of the basal spacing is obtained [25]. In step 2, physically adsorbed, intercalated, or grafted silane molecules are formed on the outer surfaces, at the broken edges, and between the adjacent layers [34,37]. As indicated by XRD, DTG, and TGA measurements (Si29 NMR was not presented to show the silicon species on solids), the mechanical mixer and homogenizer cause a double layer arrangement and lead to an increased quantity of physical adsorption and chemically bonded silane molecules compared to the other premixing processes (Fig. 4). The mechanical mixer and homogenizer also showed a higher percentage of organic aminosilane in their structures. Therefore, it can be interpreted that the homogenizer and mechanical mixer make many more molecules of water diffusion into the Na$^+$-MMT gallery and also expand the clay layers more than the other premixing processes. When the resulting Na$^+$-MMT dispersion and aminosilane solution are mixed, many more silane molecules or siloxane oligomers diffuse into the interlayer space. Accordingly, increasing the molecules of aminosilane or siloxane oligomers expands the interlayer space and provides a screening between the charges of the Na$^+$-MMT layers. Eventually, it helps the weakening of interlayer attraction and, consequently, a higher enlargement of basal spacing value [23].

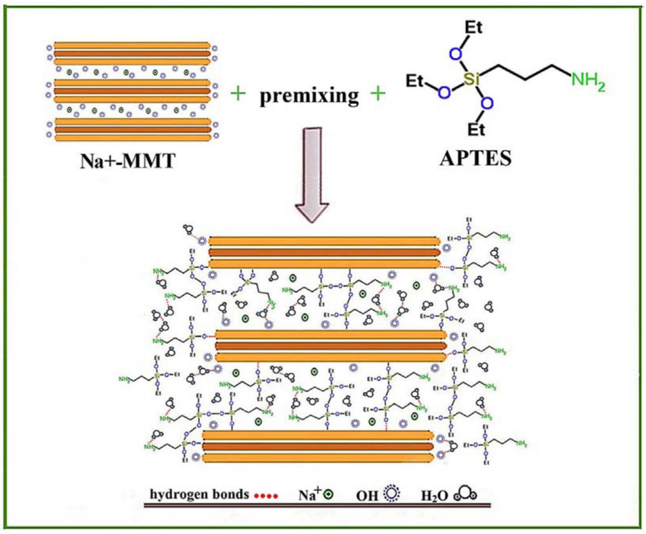

Fig. 4 Proposed structures scheme for the silylation and intercalation of APTES into Na$^+$-MMT interlayer.

Conclusions

In this research, silane-grafted Na$^+$-MMTs are synthesized with trifunctional silane (APTES), and the effects on the d-spacing and the amount of grafted aminosilane molecules of Na$^+$-MMT upon the premixing process with the different mixing techniques were studied in details. The XRD analyses show that any premixing process increases the d-spacing compared to the silylation reaction without the premixing process. Moreover, the S-Mt$_{HL}$, S-Mt$_{HH}$, and S-Mt$_{ME}$ show the presence of a double layer of aminopropyl inside the Na^{+}-MMT interlayer space. The percentage of silane loaded into the Na^{+}-MMT is calculated by the TGA. The results reveal that the S-Mt$_{HL}$, S-Mt$_{HH}$, and S-Mt$_{ME}$ show more silane in the structure. In addition, FTIR results provide further supporting evidence for the silane grafting. Our study demonstrates that the premixing process considerably influences the shift of the (0 0 1) basal spacing, the extent of grafting, and the swelling property of the silylated products. Moreover, premixing could be an important factor in the increase in the swelling property of the silylated Na^{+}-MMT and the improvement of the polymer/clay nanocomposite properties.

Acknowledgments

This study is supported by the Research Institute of Petroleum Industry; the authors would like to express their thanks to this organization.

Conflict of Interest

The authors declare that they have no conflict of interest.

References

1. Aalaie, J. (2016). viscoelastic properties of polyacrylamide nanocomposite hydrogels prepared in electrolyte media: effect of gelant volume, Journal of Petroleum Science and Technology, 6,1: 80-87. Doi:10/22078/JPST.2016.571.
2. Abbassi, H., Abidi, R., & Zayani, M. B. (2021). A short review on the silylated clays-polymer nanocomposites: synthesis, properties and applications, Moroccan Journal of Heterocyclic Chemistry, 20(2), 20-2, doi:org/10.48369/IMIST.PRSM/jmch-v20i2.24712.
3. Müller, K., Bugnicourt, E., Latorre, M., Jorda, M., Echegoyen Sanz, Y., Lagaron, J., Miesbauer, O., Bianchin, A., Hankin, S., Bölz, U., Pérez, G., Jesdinszki, M., Lindner, M., Scheuerer, Z., Castelló, S. & Schmid, M. (2017) Review on the processing and properties of polymer nanocomposites and nanocoatings and their applications in the packaging, Automotive and Solar Energy Fields Nanomater, 7(4): 74. doi: 10.3390/nano7040074.
4. Arinkoola, A. O., Atitebi, Z. M., Abidemi, G. O., Jimoh, M. O., Salam, K. K., Alagbe, S. O. & Salawudeen, T. O. (2021). Enhancement of filtration and rheological properties of water-based drilling fluid prepared using nigerian ohia bentonite and local additives, Journal of Petroleum Science and Technology, 11,4: 55-62. doi: 10.22078/JPST.2022.4644.1764.
5. Pavlidou, S. & Papaspyrides C. D. (2008) A review on polymer-layered silicate nanocomposites, Progress in Polymer Science, 33: 1119-1198. doi.org/10.1016/j.progpolymsci.2008.07.008.
6. Aalaie, J., Vasheghani-Farahani, E., Rahmatpour, A. & Semsarzadeh, M. A. (2008). Effect of montmorillonite on gelation and swelling behavior of sulfonated polyacrylamide nanocomposite hydrogels in electrolyte solutions, European Polymer Journal, 44: 2024-2031. doi: 10.1016/j.eurpolymj.2008.04.031.
7. Khoshniyat, A., Sharif, A. & Aalaie, J. (2015). Experimental and thermodynamic investigation of the stability of copolymer grafted bentonite nanoclays in a high salinity electrolyte, Polymer Science, Series A, 57: 883–888. doi: 10.1134/S0965545X1507007X.
8. Zargar, G., Firozjaii, A. M., KhedriMirghaed, M. & Moghadasi, J. (2021). Experimental study on preventing formation damage due to clay swelling caused by water based drilling fluid using aluminum ion based clay inhibitor, Journal of Petroleum Science and Technology, 11,2: 13-21, doi: 10.22078/JPST.2021.4403.1714.
9. Yan, L., Roth, C. B. & Low, P. F. (1996). Changes in the Si−O Vibrations of Smectite Layers Accompanying the Sorption of Interlayer Water, Langmuir, 12: 4421-4429. doi.org/10.1021/la960119e.
10. Toth, R., Voorn, D. J., Handgraaf, J. W., Fraaije, J. G. E. M., Fermeglia, M., Pricl, S. & Posocco, P. (2009). Multiscale Computer Simulation Studies of Water-Based Montmorillonite/Poly(ethylene oxide) Nanocomposites, Macromolecules, 42(8260-8270), doi:10.1021/ma901584w.
11. He, H., Ma, L., Zhu, J., Frost, R. L., Theng, B. K. G. & Bergaya, F. (2014). Synthesis of organoclays: A critical review and some unresolved issues, Applied Clay Science, 100(22-28), doi:10.1016/j.clay.2014.02.008.
12. He, H., Ma, Y., Zhu, J., Yuan, P. & Qing, Y. (2010) .Organoclays prepared from montmorillonites with different cation exchange capacity and surfactant configuration, Applied Clay Science, 48(67-72), doi: 10.1016/j.clay.2009.11.024.
13. Asgari, M., Abouelmagd, A. & Sundararaj, U. (2017). Silane functionalization of sodium montmorillonite nanoclay and its effect on rheological and mechanical properties of HDPE/clay nanocomposites, Applied Clay Science, 146(439-448), doi.org/10.1016/j.clay.2017.06.035.
14. Zapata, P. A., Belver, C., Quijada, R., Aranda, P. & Ruiz-Hitzky, E. (2013). Silica/clay organo-heterostructures to promote polyethylene–clay nanocomposites by in situ polymerization, Applied Catalysis A: General, 453:142. doi.org/10.1016/j.apcata.2012.12.012.
15. Bee, S. L., Abdullah, M. A .A., Mamat, M., Bee, S. T., Sin, L. T., Hui, D. & Rahmat, A. R. (2017). Characterization of silylated modified clay nanoparticles and its functionality in PMMA, Composites Part B: Engineering, 110:83-95. doi.org/10.1016/j.compositesb.2016.10.084.
16. Jincheng, W., Xiaoyu, Z., Wenli, H., Nan, X. & Xingchen, P. (2012). Synthesis of hyper-branched quaternary ammonium salt and its application into montmorillonite, Powder Technology, 221(80-89.(doi.org/10.1016/j.powtec.2011.11.006.
17. Bertuoli, P. T., Piazza, D., Scienza, L. C. & Zattera, A. J. (2014). Preparation and characterization of montmorillonite modified with 3-aminopropyltriethoxysilane, Applied Clay Science, 87(46-51). doi: 10.1016/j.clay.2013.11.020.
18. Bujdák, J., Danko, M., Chorvát, D., Czímerová, A., Sýkora, J., Lang, K. (2012). Selective modification of layered silicate nanoparticle edges with fluorophores, Applied Clay Science, 65-66(152-157), doi.org/10.1016/j.clay.2012.04.029.

19. Fatimah, I. (2018). Preparation, characterization and physicochemical study of 3-amino propyl trimethoxy silane-modified kaolinite for Pb(II) adsorption, Journal of King Saud University-Science, 30, 2(250-257), doi.org/10.1016/j.jksus.2017.04.006.
20. Majeed, K., Jawaid, M., Hassan, A., Abu Bakar, A., Abdul Khalil, H. P. S., Salema, A. A., Inuwa, I. (2013). Potential materials for food packaging from nanoclay/natural fibres filled hybrid composites, Materials & Design, 46(391-410), doi.org/10.1016/j.matdes.2012.10.044.
21. Su, L., Tao, Q., He, H., Zhu, J. & Yuan, P. (2012). Locking effect: A novel insight in the silylation of montmorillonite surfaces, Materials Chemistry and Physics, 136(292-295). doi.org/10.1016/j.matchemphys.2012.07.010.
22. He, H., Duchet, J., Galy, J. & Gerard, J. F. (2005). Grafting of swelling clay materials with 3-aminopropyltriethoxysilane, Journal of Colloid and Interface Science, 288(171-176), doi.org/10.1016/j.jcis.2005.02.092.
23. Piscitelli, F., Scamardella, A. M., Romeo, V., Lavorgna, M., Barra, G., Amendola, E. (2012), Epoxy composites based on amino-silylated MMT: The role of interfaces and clay morphology, Journal of Applied Polymer Science, 124, 1(616-628), doi.org/10.1002/app.35015.
24. Piscitelli, F., Posocco, P., Toth, R., Fermeglia, M., Pricl, S., Mensitieri & G., Lavorgna, M. (2010). Sodium montmorillonite silylation: unexpected effect of the aminosilane chain length, Journal of Colloid and Interface Science, 351(108-115), doi.org/10.1016/j.jcis.2010.07.059.
25. Ianchis, R., Corobea, M. C., Donescu, D., Rosca, I. D., Cinteza, L. O., Nistor, L. C., Vasile, E., Marin, A. & Preda, S. (2012). Advanced functionalization of organoclay nanoparticles by silylation and their polystyrene nanocomposites obtained by miniemulsion polymerization, Journal of Nanoparticle Research, 14, 11: 1233. doi: 10.1007/s11051-012-1233-6.
26. Shen, W., He, H., Zhu, J., Yuan, P., Frost, R. L. (2007). Grafting of montmorillonite with different functional silanes via two different reaction systems, Journal of Colloid and Interface Science, 313: 268-273, doi: 10.1016/j.jcis.2007.04.029.
27. Su, L., Tao, Q., He, H., Zhu, J., Yuan, P. & Zhu, R. (2013). Silylation of montmorillonite surfaces: Dependence on solvent nature, Journal of Colloid and Interface Science, 391(16-20), doi: 10.1016/j.jcis.2012.08.077.
28. Queiroga, L. N. F., Pereira, M. B. B., Silva, L. S., Silva Filho, E. C., Santos, I. M. G., Fonseca, M. G., Georgelin, T. & Jaber, M. (2019). Microwave bentonite silylation for dye removal: Influence of the solvent, Applied Clay Science, 168: 478–487. doi.org/10.1016/j.clay.2018.11.027.
29. Yang, S. q., Yuan, P., He, H. p., Qin, Z. h., Zhou, Q., Zhu, J. x. & Liu, D. (2012). Effect of reaction temperature on grafting of γ-aminopropyl triethoxysilane (APTES) onto kaolinite, Applied Clay Science, 62, 63: 8-14. doi.org/10.1016/j.clay.2012.04.006.
30. Asgari, M. & Sundararaj, U. (2018). Silane functionalization of sodium montmorillonite nanoclay: The effect of dispersing media on intercalation and chemical grafting, Applied Clay Science, 153: 228-238. doi.org/10.1016/j.clay.2017.12.020.
31. Shanmugharaj, A. M., Rhee, K. Y. & Ryu, S. H. (2006). Influence of dispersing medium on grafting of aminopropyltriethoxysilane in swelling clay materials, Journal of Colloid and Interface Science, 298: 854-859. doi: 10.1016/j.jcis.2005.12.049.
32. Ahenach, J., Cool, P., Vansant, E., Lebedev, O. & Van Landuyt, J. (1999). Influence of water on the pillaring of montmorillonite with aminopropyltriethoxysilane, Physical Chemistry Chemical Physics, 1: 3703-3708. doi.org/10.1039/A901888C.
33. Sharma, K. K., Anan, A., Buckley, R. P., Ouellette, W. & Asefa, T. (2008). Toward efficient nanoporous catalysts: controlling site-isolation and concentration of grafted catalytic sites on nanoporous materials with solvents and colorimetric elucidation of their site-isolation, Journal of the American Chemical Society, 130: 218-228, doi.org/10.1021/ja074128t.
34. Sepehri, S., Rafizadeh, M., Hemmati, M. & Bouhendi, H. (2015). Preparation of acryl amide/2-acryl amido-2-methyl propane sulfonic acid/silane modified montmorillonite water-soluble nanocomposites: study of thermal and rheological properties, Journal of Polymer Research, 22, 5: 1-11, doi: 10.1007/s10965-015-0721-7.
35. Zhao, C., Feng, M., Gong, F., Qin, H. & Yang, M. (2004). Preparation and characterization of polyethylene–clay nanocomposites by using chlorosilane-modified clay, Journal of Applied Polymer Science, 93:676-680. doi: 10.1002/app.20515.
36. Hosseinkhanli, H., Sharif, A. R., Aalaie, J., Khalkhali, T. & Akhlaghi, Sh. (2013). Oxygen Permeability, Mechanical, and Thermal Properties of LDPE/EVA/Organoclay Blown Film Nanocomposites, Journal of Vinyl and Additive Technology, 19:132-139, doi.org/10.1002/vnl.20329.
37. Silva, A. A., Dahmouche, K. & Soares, B. G. (2011). Nanostructure and dynamic mechanical properties of silane-functionalized montmorillonite/epoxy nanocomposites, Applied Clay Science, 54:151-158. doi.org/10.1016/j.clay.2011.08.002.
38. Paul, B., Martens,W. N. & Frost, R. L. (2011). Organosilane grafted acid-activated beidellite clay for the removal of non-ionic alachlor and anionic imazaquin, Applied Surface Science, 257: 5552-5558, doi.org/10.1016/j.apsusc.2011.01.034.
39. Lagaly, G. & Ziesmer, S. (2003). Colloid chemistry of clay minerals: the coagulation of montmorillonite dispersions, Advances in Colloid and Interface Science, 100, 102: 105-128. doi.org/10.1016/S0001-8686(02)00064-7.